J|A|C|S
ARTICLES

Published on Web 03/02/2009

# On the Nature of DNA Self-Assembled Monolayers on Au: Measuring Surface Heterogeneity with Electrochemical in Situ Fluorescence Microscopy

Jeffrey N. Murphy,† Alan K. H. Cheng,‡ Hua-Zhong Yu,*,‡ and Dan Bizzotto*,†

*Advanced Materials and Process Engineering Laboratory, Department of Chemistry, University of British Columbia, Vancouver, BC, Canada V6T 1Z4, and Department of Chemistry, Simon Fraser University, Burnaby, BC, Canada V5A 1S6*

Received November 5, 2008; E-mail: bizzotto@chem.ubc.ca; hogan_yu@sfu.ca

***Abstract:*** The creation of gold surfaces modified by single- or double-stranded DNA self-assembled monolayers (SAMs) is shown to produce heterogeneous surface packing densities through the use of electrochemical studies coupled with fluorescence imaging. The modified surfaces created by direct adsorption of thiolate DNA [followed by passivation with mecaptohexanol (MCH)] resulted in regions covered by a monolayer of DNA SAM and other regions that were coated by large particles of DNA. The difference in fluorescence intensity measured from these regions was dramatic. More importantly, a regional variance in fluorescence intensity in response to electrochemical potential was observed: the large aggregates showing a significantly different modulation of fluorescence intensity than the monolayer-coated regions. Electrochemical desorption and detection of the fluorescently tagged DNA provided clear evidence of a complete surface modification. These studies have implications for biosensor/biochip development using DNA SAMs. A modification in the method used to produce the DNA SAMs resulted in a significantly different surface with much fewer aggregates and more significant electromodulation of the fluorescence intensity, though at much lower DNA surface density (ca. 1% of maximum theoretical coverage). This method for forming the modified surfaces has clear advantages over the currently accepted practice and emphasizes the importance of studying the nonaveraged nature of the sensor surface using in situ imaging tools like electrofluorescence microscopy.

## 1. Introduction

Many motifs are currently proposed for the design of DNA sensors.[1,2] Among these is the creation of a DNA sensor that couples DNA to a surface, allowing either electrochemical or spectroscopic transduction of binding events. The creation of these DNA-modified surfaces has employed thiol−Au self-assembly and was popularly adapted.[3−5] Briefly, the 5′-alkylthiol-modified DNA was tethered to the Au surface in the self-assembled monolayer (SAM) modality, and nonspecific adsorption of DNA (i.e., through base pair adsorption onto the Au) was prevented or DNA was removed through the subsequent treatment with mercaptohexanol (MCH). The introduction of MCH would compete for these adsorption sites, displacing the nonspecifically adsorbed DNA, presumably resulting in a SAM of DNA and MCH that were thoroughly mixed and homogeneous, though indirect evidence of their heterogeneity was recently reported[6] for these mixed SAMs. This same method was used to create surfaces that contained DNA with fluorescent tags on the 3′-terminus, which is furthest from the metal surface. A number of studies have been reported using fluorescently tagged DNA SAMs for sensors.[7−14] Interestingly, variation in the potential of the Au surface was used to manipulate the DNA orientation so that the strands were either standing up or lying down, resulting in strong changes in the fluorescence[9] exploiting

† University of British Columbia.
‡ Simon Fraser University.

(1) Drummond, T. G.; Hill, M. G.; Barton, J. K. *Nat. Biotechnol.* **2003**, *21*, 1192–1199.
(2) Tarlov, M. J.; Steel, A. B. *Surfactant Sci. Ser.* **2003**, *111*, 545–608.
(3) Herne, T. M.; Tarlov, M. J. *J. Am. Chem. Soc.* **1997**, *119*, 8916–8920.
(4) Steel, A. B.; Herne, T. M.; Tarlov, M. *J. Anal. Chem.* **1998**, *70*, 4670–4677.
(5) Levicky, R.; Herne, T. M.; Tarlov, M. J.; Satija, S. K. *J. Am. Chem. Soc.* **1998**, *120*, 9787–9792.
(6) Lao, R.; Song, S.; Wu, H.; Wang, L.; Zhang, Z.; He, L.; Fan, C. *Anal. Chem.* **2005**, *77*, 6475–6480.
(7) Takeishi, S.; Rant, U.; Fujiwara, T.; Buchholz, K.; Usuki, T.; Arinaga, K.; Takemoto, K.; Yamaguchi, Y.; Tornow, M.; Fujita, S.; Abstreiter, G.; Yokoyama, N. *J. Chem. Phys.* **2004**, *120*, 5501–5504.
(8) Rant, U.; Arinaga, K.; Fujita, S.; Yokoyama, N.; Abstreiter, G.; Tornow, M. *Nano Lett.* **2004**, *4*, 2441–2445.
(9) Rant, U.; Arinaga, K.; Fujita, S.; Yokoyama, N.; Abstreiter, G.; Tornow, M. *Langmuir* **2004**, *20*, 10086–10092.
(10) Rant, U.; Arinaga, K.; Tornow, M.; Kim, Y. W.; Netz, R. R.; Fujita, S.; Yokoyama, N.; Abstreiter, G. *Biophys. J.* **2006**, *90*, 3666–3671.
(11) Rant, U.; Arinaga, K.; Scherer, S.; Pringsheim, E.; Fujita, S.; Yokoyama, N.; Tornow, M.; Abstreiter, G. *Proc. Natl. Acad. Sci. U.S.A.* **2007**, *104*, 17364–17369.
(12) Arinaga, K.; Rant, U.; Knezevic, J.; Pringsheim, E.; Tornow, M.; Fujita, S.; Abstreiter, G.; Yokoyama, N. *Biosens. Bioelectron.* **2007**, *23*, 326–331.
(13) Tornow, M.; Arinaga, K.; Rant, U. Electrical Manipulation of DNA on Metal Surfaces. In *NanoBioTechnology, BioInspired Devices and Materials of the Future*; Shoseyov, O., Levy, I., Eds.; Humana Press: Totowa, NJ, 2008; pp 187−214.
(14) Sendner, C.; Kim, Y. W.; Rant, U.; Arinaga, K.; Tornow, M.; Netz, R. R. *Phys. Status Solidi A* **2006**, *203*, 3476–3491.

 **10.1021/ja808696p CCC: $40.75** 

the distance-dependent quenching of fluorescence by the metal surface.[15] Despite these findings, a number of questions remained unanswered, specifically addressing the issue of hybridization efficiency,[16,17] which have been addressed in many ways such as decreasing the DNA surface density.

One important parameter, though difficult to quantify, is the nature of the modified surface and its degree of homogeneity in terms of surface density, which is typically characterized by measuring the Faradaic current due to penetration of redox probes through the defects in the SAM (see, for example, refs 18, 19) among many other methods. Unfortunately, these techniques typically report an average picture of the interface. We will illustrate the utility of an electrochemical fluorescence imaging method developed recently[20−22] for interrogating a modified electrode surface. We will use the changes in fluorescence intensity with potential to specifically address the issue of surface heterogeneity of SAMs created from fluorescently tagged DNA. In addition, we will show an alternative DNA SAM preparation method that has the potential to improve the quality of the sensor surface, ensuring a much improved transduction for given binding events.

## 2. Experimental Section

**2.1. Sample Preparation.** Gold beads of approximately 1−2.5 mm in diameter were used as substrates after cleaning with warm "piranha" [concentrated $H_2SO_4$:$H_2O_2$ (30%)/3:1 v/v] solution (**CAUTION**: piranha solution is a strong oxidant and must be used with care), rinsing in DI water, and flame annealing. The modification of the gold beads by a SAM of DNA follows literature reports.[3,4,7,23] Briefly, purified single-stranded (ss) DNA solutions [obtained from Sigma-Genosys, with sequences HO−$(CH_2)_6$−S−S−$(CH_2)_6$−O−5′-CTG TAT TGA GTT GTA TCG TGT GGT GTA TTT-[CY3]-3′ (LN1) or HO−$(CH_2)_6$−S−S−$(CH_2)_6$−O−5′-GTT GTG GCC AAG TAC AAA TTA TGG TAT CTA-[CY5]-3′ (LN5); unlabeled complementary sequences were obtained from University Core DNA Services, University of Calgary] were reduced using tris(2-carboxyethyl)phosphine hydrochloride and purified using MicroSpin G50 columns. The solutions were then diluted to approximately 1 $\mu$M in an immobilization buffer containing 10 mM Tris, with added NaCl (100 mM) and $MgCl_2$ (500 mM) (similar heterogeneous surfaces were obtained with a range of [NaCl] = 10−1000 mM and [$MgCl_2$] = 0−500 mM). The gold beads were then placed in a 20 $\mu$L drop of the DNA solution in an Eppendorf tube, sealed, wrapped in aluminum foil to prevent photobleaching, and incubated for times ranging up to 24 h at room temperature. When double-stranded (ds) DNA was used, the deposition solution is made to the same concentrations, with the addition of an equal concentration of the complementary ssDNA strand, and the strands were annealed at 70−80 °C and then cooled over 1 h.

Following DNA deposition, the beads are rinsed with fresh immobilization buffer solution, followed by deionized water. The surface was then treated with MCH (1 mM) in the immobilization buffer for 1 h, rinsed with deionized water, and then stored in a fresh solution of the immobilization buffer in the dark. These are further referenced as DNA/MCH samples. The surface density of tethered DNA was determined by CV measurements using $[Ru(NH_3)_6]^{3+}$ as a reporter molecule following literature reports.[24,25] Briefly, the coated beads were rinsed with Millipore water and then immersed in deareated $[Ru(NH_3)_6]^{3+}$ solutions [5 $\mu$M in a 10 mM Tris buffer solution (pH ∼7.5)] for 15 min to equilibrate. The DNA surface concentration was determined by integration of the redox peaks for DNA-bound $[Ru(NH_3)_6]^{3+}$. The modified Au surfaces were then characterized using electrochemical and spectroscopic techniques after immersion in immobilization buffer to remove the bound $[Ru(NH_3)_6]^{3+}$.

**2.2. Electrochemistry and Fluorescence Microscopy.** The modified Au beads were further studied using a methodology described previously which allows for in situ fluorescence imaging of the electrode surface during potential perturbations. This method has been used to examine the potential induced behavior of adsorbed lipids and fluorescent thiol molecules.[20,22] The fluorescence measured were from Au beads that were flame annealed before modification; such smooth surfaces are not candidates for fluorescence enhancement, as reported by Lakowicz.[26] Briefly, the gold bead is used as the working electrode in a three-electrode arrangement [a Au coil counter electrode and SCE reference in an electrolyte composed of 10 mM Tris and 10 mM $NaBF_4$ (Fluka)] in a specially constructed spectroelectrochemical cell that allows for imaging with an inverted epifluorescence microscope (Olympus IX70) equipped with a U-MNG2 filter cube [excitation filter (530−550 nm), a dichroic mirror (570 nm), and an emission band-pass filter (>590 nm)] (see Supporting Information for an experimental schematic). Cyclic voltammetry and differential capacitance measurements were performed on the bead electrode concurrent with fluorescence imaging. The fluorescence images were acquired with a 20× (NA = 0.4) objective and a SPOT RT camera, resulting in images with a resolution of 1 pixel per micrometer. The images were analyzed using ImageJ[27] and the image intensities were normalized with respect to exposure time and reported as the average counts per second (cps) per pixel. The fluorescence images presented were acquired during a potential step program. The potential was stepped from a base potential ($E_{base}$ = 0 mV vs SCE) to various step potentials ($E_{step}$). The capacitance was measured as well as five fluorescence images at each potential. The $E_{step}$ potentials started at 0 mV vs SCE and were made progressively more negative by 25 mV until a predetermined negative limit (usually −1.250 V vs SCE) was reached.

## 3. Results and Discussion

**3.1. DNA/MCH Surfaces: Images at Open Circuit Potential (OCP).** Numerous DNA-modified Au surfaces were produced following the procedure described by Herne and Tarlov.[3] The fluorescence and capacitance changes as a function of potential were measured for each of these surfaces. The samples were composed of ssDNA or dsDNA self-assembled monolayer (SAM) modified gold surfaces which were passivated by exposure to an MCH solution to remove nonspecifically adsorbed DNA. Surfaces created this way contained ∼1 × $10^{13}$ strands per $cm^2$ and 0.5 × $10^{13}$ strands per $cm^2$, respectively (measured with CV/CC studies of surface-bound $[Ru(NH_3)_6]^{3+}$), similar to that reported in the literature for similar assembly procedures.[3] A representative selection of fluorescence images

(15) Chance, R. R.; Prock, A.; Silbey, R. Molecular fluorescence and energy transfer near interfaces. In *Advances in Chemical Physics*; Prigogine, I., Ed.; Interscience Publishers: New York, 1978; Vol. 37, pp 1−65.
(16) Levicky, R.; Horgan, A. *Trends Biotechnol.* **2005**, *23*, 143–149.
(17) Spitzer, J. J.; Poolman, B. *Trends Biochem. Sci.* **2005**, *30*, 536–541.
(18) Badia, A.; Lennox, R. B.; Reven, L. *Acc. Chem. Res.* **2000**, *33*, 475–481.
(19) Love, J. C.; Estroff, L. A.; Kriebel, J. K.; Nuzzo, R. G.; Whitesides, G. M. *Chem. Rev.* **2005**, *105*, 1103–1169.
(20) Shepherd, J. L.; Kell, A.; Chung, E.; Sinclar, C. W.; Workentin, M. S.; Bizzotto, D. *J. Am. Chem. Soc.* **2004**, *126*, 8329–8335.
(21) Bizzotto, D.; Shepherd, J. L. *Adv. Electrochem. Sci. Eng.* **2006**, *9*, 97–126.
(22) Musgrove, A.; Kell, A.; Bizzotto, D. *Langmuir* **2008**, *24*, 7881–7888.
(23) Ge, B.; Huang, Y. C.; Sen, D.; Yu, H. Z. *J. Electroanal. Chem.* **2007**, *602*, 156–162.
(24) Yu, H. Z.; Luo, C. Y.; Sankar, C. G.; Sen, D. *Anal. Chem.* **2003**, *75*, 3902–3907.
(25) Su, L.; Sankar, C. G.; Sen, D.; Yu, H. Z. *Anal. Chem.* **2004**, *76*, 5953–5959.
(26) Lakowicz, J. R. *Anal. Biochem.* **2005**, *337*, 171–194.
(27) Rasband, W. S. *ImageJ Documentation*.

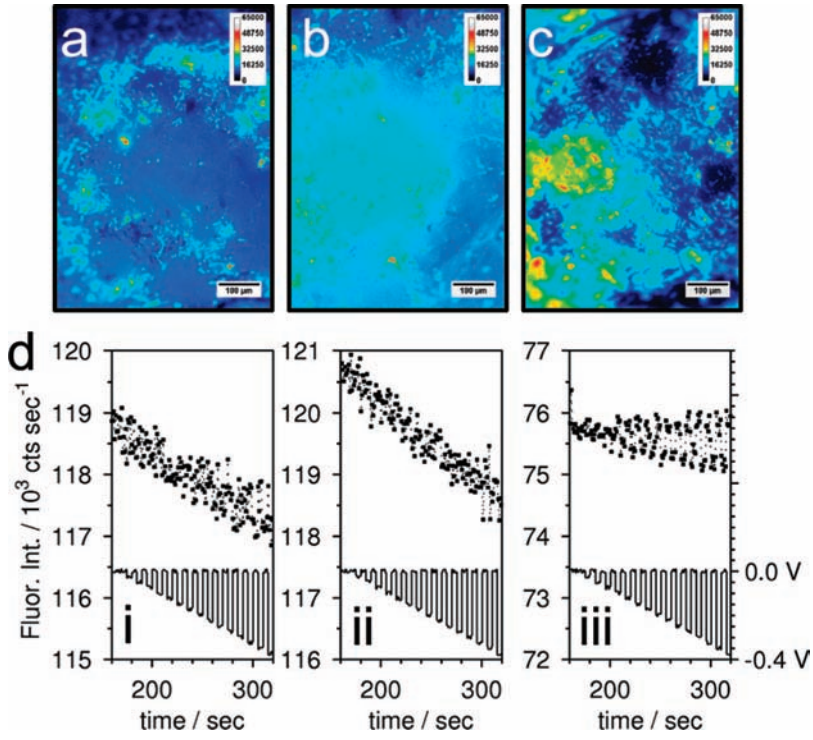


***Figure 1.*** Fluorescence images of gold surfaces modified by (a) ssDNA/MCH, (b) another example of a ssDNA/MCH layer, and (c) dsDNA/MCH imaged in an electrochemical cell at open circuit potential. (d) the corresponding change in fluorescence measured during sequential potential steps from 0 to −400 mV for the surfaces (i) a, (ii) b, and (iii) c. The ssDNA/MCH sample images were taken with 0.1 s exposure time, while the dsDNA image was taken with 0.2 s exposure time. The intensity of fluorescence is rendered as a range of colors, shown in the color−intensity bar.

measured at OCP (i.e., unbiased) are shown for two similarly prepared ssDNA-modified surfaces (Figure 1a,b) and a dsDNA-modified surface (Figure 1**c**). In the majority of cases, as illustrated by these two examples, the measured fluorescence is not uniformly distributed and small local regions appear particularly fluorescent. This heterogeneity in fluorescence suggests a similar heterogeneity in DNA packing density. The clusters of intense fluorescence are tens of square micrometers and cover 10−30% of the surface. Fluorescence of this magnitude ($\sim 10^6$ cps) is usually observed for the fluorescent moiety far from the gold surface (e.g., as a floating monolayer), suggesting that these areas represent a significant amount of DNA that may be aggregating on the surface with a large fraction of the strands located far from the surface, i.e., untethered or nonspecifically adsorbed in a form that we speculate is crystalline in nature.[28−30] In general, the ssDNA surface has many more of these "hot spots" as compared to the dsDNA surface, further supporting the formation of DNA crystallites, as dsDNA is less prone to aggregation compared to ssDNA.[31]

**3.2. DNA/MCH Surfaces: Potential Modulation (0 to −400 mV vs SCE).** DNA-modified surfaces form the basis for DNA microarray technology.[32−34] The use of gold substrates enables the use of potential-controlled modulation of the fluorescence intensity, which reports on the changes in hybridization, conferring a unique advantage in this electrochemical approach. Changes in the orientation of either ssDNA or dsDNA is dependent on the potential of the Au substrate, as shown using AFM,[35] SPR,[36] and fluorescence spectroscopy.[8,10] At positive potentials, the DNA is attracted to the surface (decreasing fluorescence), while at negative potentials the DNA is repelled from the surface, increasing fluorescence. The magnitude, or rate, of fluorescence modulation has been suggested to be used as the transduction modality; though it is quite dependent on the density of DNA coverage, the modulation amplitude decreases as the DNA surface concentration increases.

The heterogeneous surfaces shown in Figure 1 were characterized by measuring the changes in the fluorescence intensity of the adsorbed DNA during potential perturbations. At first the potential excursions are kept to a restricted region, starting at 0 mV and stepping to values between 0 and −400 mV, specifically to investigate the changes in fluorescence due to potential modulated orientation changes in the adsorbed DNA. This data is shown in Figure 1d(i, ii, iii) for the three samples (a, b, c), respectively. The change in the average fluorescence intensity as compared to 0 mV ($E_{base}$) is shown along with changes in potential. No modulation was observed for the ssDNA surfaces with high surface densities. The magnitude of the oscillation (<2% of overall fluorescence) is small and only observed for the lower surface concentration dsDNA sample. In addition, a constant decrease in fluorescence was observed, suggesting a reorganization or loss of the surface species or a photobleaching process.

(28) Nakata, M.; Zanchetta, G.; Chapman, B. D.; Jones, C. D.; Cross, J. O.; Pindak, R.; Bellini, T.; Clark, N. A. *Science* **2007**, *318*, 1276–1279.
(29) Bloomfield, V. A. *Biopolymers* **1997**, *44*, 269–82.
(30) Wong, K.; Pettitt, B. M. *Theor. Chem. Acc.* **2001**, *106*, 233–235.
(31) Burak, Y.; Ariel, G.; Andelman, D. *Biophys. J.* **2003**, *85*, 2100–2110.
(32) Wong, E. L. S. *Biophys. Rev. Let.* **2007**, *2*, 167–189.
(33) Wang, J. *Biosens. Bioelectron.* **2006**, *21*, 1887–1892.
(34) Li, C.; Long, Y.; Sutherland, T.; Lee, J. S.; Kraatz, H. B. *Front. Biochip Technol.* **2006**, 274–291.
(35) Kelley, S. O.; Barton, J. K.; Jackson, N. M.; McPherson, L. D.; Potter, A. B.; Spain, E. M.; Allen, M. J.; Hill, M. G. *Langmuir* **1998**, *14*, 6781–6784.
(36) Yang, X.; Wang, Q.; Wang, K.; Tan, W.; Yao, J.; Li, H. *Langmuir* **2006**, *22*, 5654–5659.

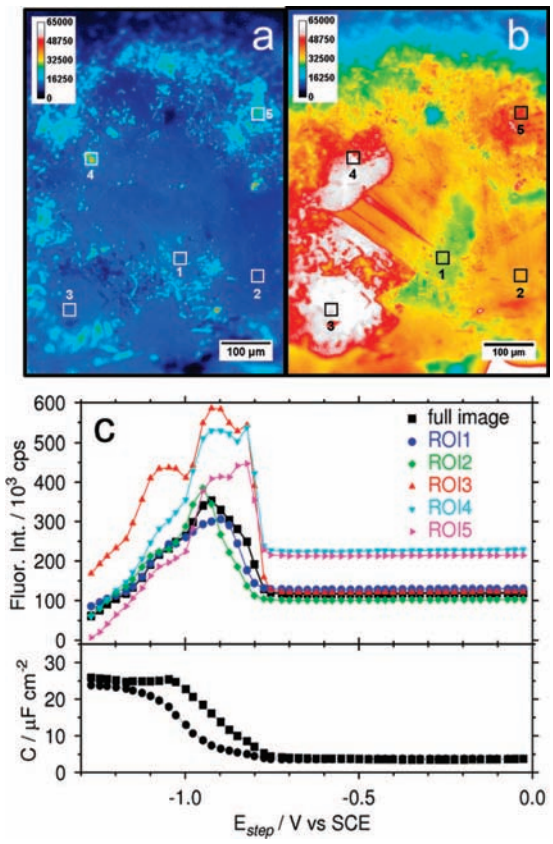


***Figure 2.*** Fluorescence images for the ssDNA/MCH modified gold surface at (a) $E_{base}$ (0 mV) and (b) maximum of the $E_{step}$ images during desorption. (c) Fluorescence intensity (top) measured (at $E_{step}$) for the whole image and selected ROIs (50 $\mu$m × 50 $\mu$m), and capacitance (bottom) measured at $E_{step}$ (■) and $E_{base}$ (●) after the $E_{step}$ potential excursion. The intensity of fluorescence is rendered as a range of colors, shown in the color−intensity bar.

**3.3. DNA/MCH Surfaces: Reductive Desorption.** Measurement of the DNA coverage was performed by electrochemically removing (via reduction) the fluorescent DNA layer while simultaneously monitoring fluorescence and capacitance. This follows our previous electrochemical study of SAMs composed of fluorescently labeled alkylthiols,[20,22] where fluorescence images were recorded during reductive desorption potential step experiments. The average fluorescence intensities of the ssDNA surfaces shown in Figure 1a were measured as a function of the negative $E_{step}$ potential for the whole image and for specific regions of interest (ROIs) of 50 $\mu$m × 50 $\mu$m, shown in Figure 2. The fluorescence image at $E_{base}$ (Figure 2a) shows regions of low (ROI 3) and high (ROI 4 and 5) fluorescence. The potential is then stepped to increasingly negative values and the adsorbed layer is reductively desorbed, diffusing away from the electrode surface. Figure 2b shows the maximum fluorescence intensity measured from each pixel during this negative potential excursion. The fluorescence intensity for each ROI and the whole image in addition to the capacitance measured for the whole surface as a function of $E_{step}$ is shown in Figure 2c. The features in this fluorescence image clearly show that the nature of the underlying surface of Au influences this process. At a potential of −775 mV, desorption of a portion of the surface commences, clearly showing the grain boundaries and surface structure of the underlying Au substrate (a movie of this desorption is available as Supporting Information). We have previously confirmed using in situ fluorescence imaging[20] that Au(111) desorbs at the least negative potential, which may also be the case here. The capacitance also starts to increase at −775 mV, indicating the start of desorption. Nevertheless, the long narrow features that are present in the center of the image and the two large regions on the left of the image and the region at the top right desorb first, followed by the region on the lower right. This is also clearly observed in the intensity vs $E_{step}$ plots (Figure 2c, top panel) and somewhat in the capacitance changes with $E_{step}$.

The heterogeneity of the substrate surface plays a role in the desorption behavior, but the intensity of the fluorescence observed when the SAM is desorbed should reflect the amount of DNA present in these regions, given that the fluorescence quenching by the surface is ineffective once separated from the surface. As expected, ROI 4 and 5 show the largest maximum fluorescence signal, with an absolute increase of 250 kcps or an increase by 2−2.5 times. Regions with intermediate $E_{base}$ fluorescence (ROI 1 and 2) increase to the same absolute extent (250 kcps) but proportionally increase by a factor of 2.5−3. The region with an intermediate $E_{base}$ fluorescence (ROI 3) shows the largest increase (∼450 kcps) or a factor of 5. It is clear that the surface is covered with the DNA SAM as every region displays an increase in fluorescence as the reductive desorption of the thiol drives the produced thiolate away from the Au surface, decreasing the quenching efficiency of Au, resulting in a fluorescence increase. At large enough negative $E_{step}$, the surface is devoid of thiol and the intensity falls or trends to zero in all regions, clearly illustrating the extent of the small background signal. In addition, the capacitance also confirms removal of the adsorbed organic layer, yielding capacitance values that are representative of the bare gold electrode.[37]

Measurement of the proportional increase in fluorescence compensates for differences in DNA packing densities if the adsorbed layer is uniform in orientation and initial quenching efficiency. The change in fluorescence observed as a function of $E_{step}$ is not uniformly distributed across the surface, as clearly demonstrated through a measure of the proportional changes. If the amount of DNA adsorbed were similar across the surface, then the overall fluorescence increase when desorbed should be similar, but this too is dependent on the initial fluorescence measured. The initial adsorbed layer must contain DNA that is adsorbed so as to be further from the Au surface giving a greater $E_{base}$ fluorescence and a smaller proportional increase in fluorescence due to desorption, something that would be expected for physisorbed DNA on top of the DNA SAM layer.

Similar conclusions can be reached for the dsDNA-modified surface, though the number of high fluorescence regions is reduced. The $E_{base}$ and maximum $E_{step}$ images and fluorescence intensity data are shown in parts a, b, and c of Figure 3, respectively. At $E_{base}$ (0 mV), the surface is not uniformly fluorescent, showing many dark regions, though Figure 3b shows that the surface is fully modified by the DNA SAM. Therefore, the dark regions contain DNA that are oriented so that the fluorescence is efficiently quenched. Performing the same regional analysis shows that the stronger fluorescing regions at $E_{base}$ have a fluorescence increase at desorption that is proportionally smaller than darker regions. For example, compare ROI 2 with an increase of 2 times to ROI 1 with an increase of 4−5

(37) Lipkowski, J.; Stolberg, L. Molecular Adsorption at Gold and Silver Electrodes. In *Adsorption of Molecules at Metal Electrodes*; Lipkowski, J., Ross, P. N., Eds.; VCH: New York, 1992; pp 171−238.

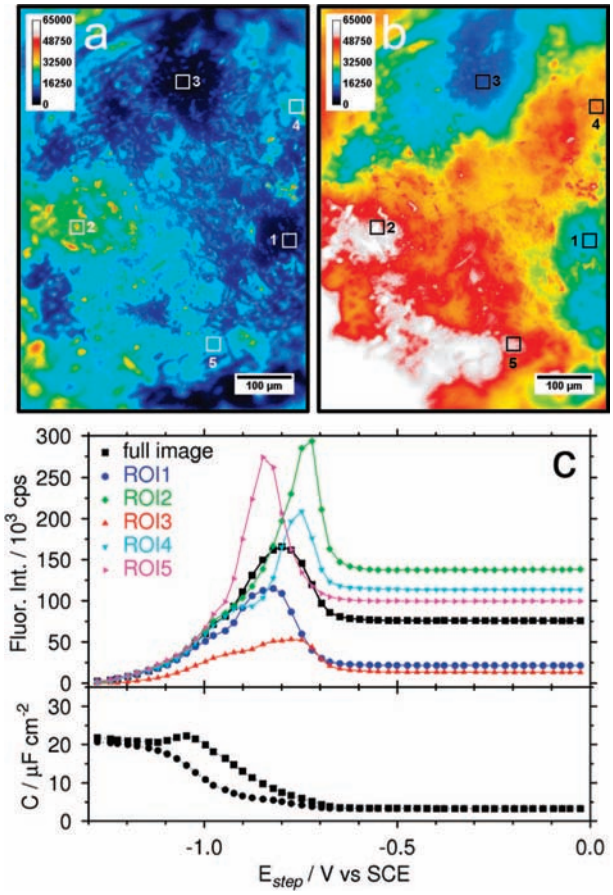


***Figure 3.*** Fluorescence images for the dsDNA/MCH-modified gold surface at (a) $E_{base}$ (0 mV) and (b) maximum of the $E_{step}$ images during desorption. (c) Fluorescence intensity (top) measured (at $E_{step}$) for the whole image and selected ROIs (50 $\mu$m × 50 $\mu$m), and capacitance (bottom) measured at $E_{step}$ (■) and $E_{base}$ (●) after the $E_{step}$ potential excursion. The intensity of fluorescence is rendered as a range of colors, shown in the color−intensity bar.

times. Once again, at large negative $E_{step}$ values, all the DNA is removed from the surface and the fluorescence measured is at background levels (<1 kcps). The capacitance at the negative $E_{step}$ potentials shows complete removal of the DNA/MCH SAM. The nonspecific adsorption of dsDNA appears to occupy a lower percentage of the surface when compared to the ssDNA example, though the influence on the fluorescence is the same: larger initial $E_{base}$ fluorescence results in proportionally smaller increases in fluorescence during desorption. Again, this can be explained through the presence of nonspecifically adsorbed DNA, which exists further from the metal surface.

Interestingly, the capacitance for the ssDNA- and dsDNA-modified surfaces shows a slight difference in the potential where the layer begins to desorb (−725 and −675 mV vs SCE, respectively) The desorption as measured by fluorescence starts at −650 mV vs SCE for dsDNA and at −775 mV vs SCE for the ssDNA sample. The capacitance is sensitive to both the adsorbed DNA and MCH over the whole surface, while fluorescence reports on the labeled DNA when removed from the electrode surface. This difference in the initial desorption potential may be a consequence of the smaller packing density of the dsDNA as compared to the ssDNA or as a result of fewer interactions between the gold surface and base pairs in dsDNA.

Patchy fluorescence features are observed for the dsDNA-modified surface in the images at $E_{base}$ (Figure 3a). Image

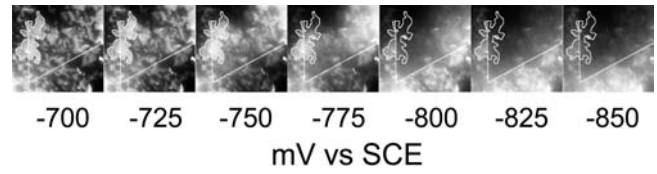


***Figure 4.*** Fluorescence images of a specific region of the dsDNA/MCH layer during a desorption potential step routine. The images (250 $\mu$m × 250 $\mu$m) are taken at $E_{step}$ potentials indicated. A feature is outlined to illustrate the reductive removal of only one portion of the feature, dependent upon the underlying surface organization. The grain boundary outlining the surface facet is outlined as well.

analysis shows that these regions are not correlated to the underlying gold surface structures. This is clearly demonstrated by looking at the desorption process in a particular region from Figure 3 shown magnified in Figure 4 for a collection of $E_{step}$ potentials. The fluorescence image appears patchy and clearly shows domains of fluorescent and nonfluorescent DNA. Outlined in the images is a fluorescent region that is also observed at 0 mV vs SCE. At a specific potential, a portion of this region is desorbed, delineated by a straight edge, which is representative of the underlying gold surface structure. In fact, further analysis shows that the desorbed region outlines a 63° grain boundary, as indicated in the figure, as expected for a Au(111) facet, something we have shown will desorb at the least negative potential. The image appears somewhat diffuse, but this is due to the fluorescing desorbed thiolate moving over and interfering with adjacent regions, resulting in a diffusing plume of fluorescence. The modification of the gold bead by self-assembly of thiolate DNA and MCH is independent of the underlying gold surface structure and seems to be dominated by the intermolecular interactions rather than the thiol interaction with the gold surface.

For ssDNA/MCH- and dsDNA/MCH-modified surfaces studied, regional image analysis of the reductive desorption process reveals that the changes in fluorescence are largest at the hot spots, but the percentage change in the fluorescence as compared to the fluorescence at $E_{base}$ is greatest away from the hot spots. If the thiolate is fully separated from the gold surface when desorbed, the fluorescence intensity must be similar across the surface for similar DNA densities, unless the final measured intensity is a measure of the local surface concentration of DNA. The regions that fluoresce at $E_{base}$ must have the fluorophore further from the gold surface than the dark regions. The degree of quenching depends nonlinearly on the distance from the gold surface; therefore, a large percentage increase reveals that each region may have a different starting point on the quenching curve, which suggests that the adsorbed layer is different in different regions such that the fluorophore is further from the gold surface. The logical explanation is that the DNA is physisorbed or nonspecifically adsorbed to the surface or is present as a large crystalline mass with a larger than expected separation from the gold at $E_{base}$. It is clear that the surface created using these methods suffers greatly from the heterogeneity in surface packing density; this must be significant, given that these surfaces are to be used as sensors. The characterization method of fluorescence imaging coupled with electrochemical control is uniquely positioned to address these issues of surface heterogeneity, and we suggest that a number of experiments in the current literature might be revisited with these findings in mind.

**3.4. MCH/DNA Surfaces.** The surfaces created following the direct self-assembly procedure rely upon the treatment of the

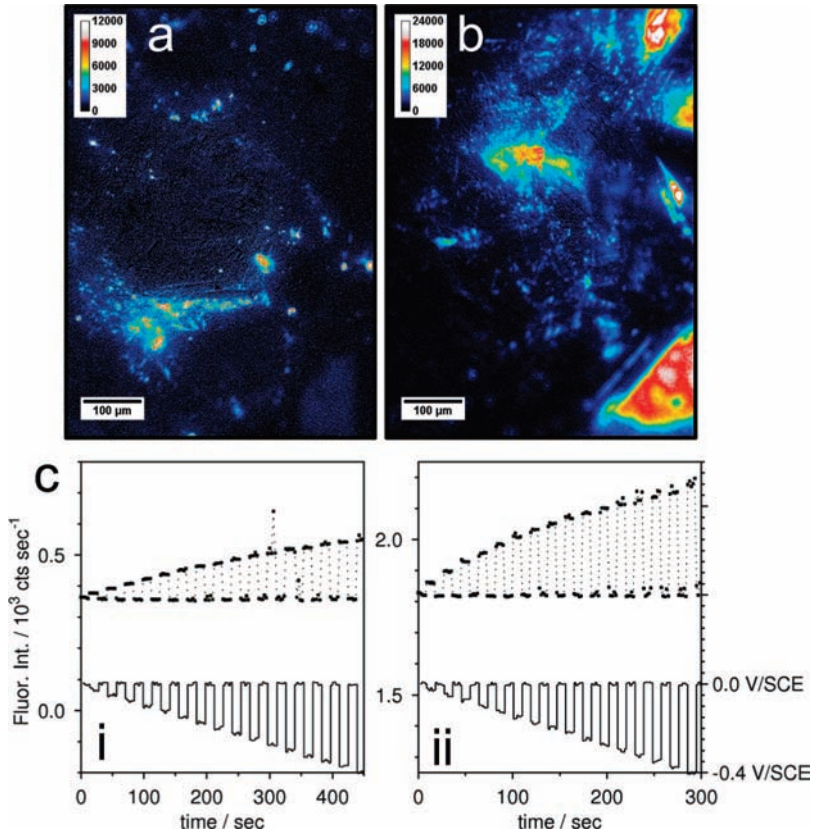


***Figure 5.*** Fluorescence images of gold surfaces modified by (a) MCH/ssDNA and (b) MCH/dsDNA imaged in an electrochemical cell at open circuit potential. (c) the corresponding change in fluorescence measured during sequential potential steps from 0 to −400 mV corresponding to (i) a and (ii) b, respectively. The MCH/ssDNA and MCH/dsDNA sample images were acquired with a 2.5 and a 1.5 s exposure time, respectively. The intensity of fluorescence is rendered as a range of colors, shown in the color−intensity bar.

DNA SAM-modified gold surface with MCH to remove nonspecifically bound DNA (physisorbed through bases). These surfaces show significant heterogeneity, which may be due to physisorbed DNA or to aggregated DNA adsorbed from solution, as demonstrated above. In either case, the reductive desorption measurements show that the adsorbed DNA strands can be removed using negative potentials. In our hands, we were never able to produce surfaces that were free of these hot spots. Decreasing the initial DNA deposition time to 30 min does eliminate the hot spots to a large extent and allows for a greater modulation of fluorescence between 0 and −400 mV. Control over the surface density is difficult, as expected from previous studies of SAM formation.[19,38]

To further investigate the origin and nature of these hot spots and the resulting nonuniform coverage, the surface modification procedure was modified by creating DNA SAM-covered surfaces with fewer hot spots and with a well-controlled but much lower DNA concentration. The Au surface was first treated with MCH for 60 min and then exposed to the thiolate DNA solution for up to 24 h. We expect that the thiolated DNA would populate the surface by way of a thiol-exchange process and/or through defects in the MCH SAM, both of which are influenced by the underlying Au surface.[19,39,40] This procedure differs from those in the literature,[41,42] which create a defective thiol SAM on Au and subsequently incorporate DNA into the defect areas. The possibility for DNA to nonspecifically adsorb is greatly reduced given that the surface was covered with a MCH SAM layer, but the adsorption of small DNA crystallites is still possible, as these result mainly from precipitation or aggregation events near or on a surface.[43] Representative fluorescence images measured at OCP are shown for ssDNA- and dsDNA-modified surfaces in Figure 5, parts a and b, respectively, at OCP. The DNA surface density for these samples are $1.1 \times 10^{10}$ and $3.7 \times 10^{10}$ strands per $cm^2$ or ∼100−1000 times smaller than the samples prepared by the previous protocol, resulting in a fluorescence yield that was also substantially lower (by ∼100−200 times). For these low-intensity fluorescence images, leakage of the excitation light through the filters becomes a problem, and therefore, the final desorption potential $E_{base}$ image was subtracted so as to compensate for the background contribution. The fluorescence images again appear nonuniform with small regions of high fluorescence and regions of more diffuse fluorescence. The ssDNA and dsDNA surfaces demonstrate the preferential exchange reaction occurring on particular facets of the Au surface. In the dsDNA surface, a region in the bottom right is more fluorescent than other regions, suggesting an increase in the DNA surface concentration. This is particularly evident for the dsDNA surface, where various

(38) Erts, D.; Polyakov, B.; Olin, H.; Tuite, E. *J. Phys. Chem. B* **2003**, *107*, 3591–3597.
(39) Caragheorgheopol, A.; Chechik, V. *Phys. Chem. Chem. Phys.* **2008**, *10*, 5029–5041.
(40) Baralia, G. G.; Duwez, A.; Nysten, B.; Jonas, A. M. *Langmuir* **2005**, *21*, 6825–6829.
(41) Aqua, T.; Naaman, R.; Daube, S. S. *Langmuir* **2003**, *19*, 10573–10580.
(42) Satjapipat, M.; Sanedrin, R.; Zhou, F. *Langmuir* **2001**, *17*, 7637–7644.
(43) Lee, A. Y.; Ulman, A.; Myerson, A. S. *Langmuir* **2002**, *18*, 5886–5898.

features that are indicative of the underlying Au surface become visible. Again, many more highly fluorescent specks are observed for the ssDNA surface when compared to the dsDNA surface, similar to results from the previous preparation procedure.

**3.5. MCH/ssDNA Potential Modulation from 0 to −400 mV.** The presence of intense fluorescence regions or specks may indicate a local increase in DNA concentration or possible small nonspecifically adsorbed crystallites (ROI 1 and 2). Regions with lower and more diffuse fluorescence (ROI 3 and 4) show a larger proportional change in fluorescence modulation with changes in potential. The average change in fluorescence due to potential modulation between 0 and −400 mV is shown in Figure 5c for both surfaces. The extent of modulation is much greater than observed for the DNA/MCH samples, with no indication of decay in the fluorescence intensity with time. This is in agreement with the electrochemically modulated fluorescence results reported by Rant and co-workers[8,11,13] Not shown are the regional differences in the percent modulation. As demonstrated for the DNA/MCH surfaces, the regions with the lowest $E_{base}$ fluorescence show modulation equivalent to the $E_{base}$ fluorescence (ROI 3 and 4). Modulation for the highly fluorescent region (ROI 1 and 2) is <10% and a small consistent decrease in $E_{base}$ fluorescence is also noted with potential stepping. It appears that the extent of modulation depends on the surface density and it is expected that lower $E_{base}$ fluorescence should correlate with lower DNA coverage and larger modulation. The higher $E_{base}$ fluorescence and low modulation is indicative of either a highly concentrated region of DNA either as a crystallite or a region with a large surface concentration. (The extent of fluorescence modulation for various regions is shown in the Supporting Information.)

**3.6. MCH/ssDNA Reductive Desorption.** Relative changes in the fluorescence increase upon desorption from the electrode surface show the differences between the different regions. Increases in fluorescence intensity and capacitance indicate that the reductive desorption of the MCH/ssDNA surface began at −625 mV, which is 150 mV more positive than the corresponding ssDNA/MCH layer (data is shown in Figure 6c). As observed in the other samples, the changes in fluorescence with potential fall into two categories: large $E_{base}$ fluorescence results in small proportional change when desorbed, and low $E_{base}$ fluorescence is related to the higher proportional fluorescence change. The two most intense regions (ROI 1 and 2) do not show large increases in fluorescence intensity during desorption (above the maximum in fluorescence due to modulation). This may be due to the elongation of DNA to its full extent so that the fluorophore is fully separated from the electrode surface such that it is almost completely fluorescent and the resulting increase in fluorescence due to desorption is minor. Alternatively, these regions show characteristics observed in the ssDNA/MCH samples that we assigned to physisorbed DNA. The weaker fluorescence regions do show the usual increase in fluorescence intensity during desorption that are 3−4 times the initial fluorescence. In all cases the electrode surface is fluorescently dark after complete desorption.

The maximum intensity fluorescence image (Figure 6b) for the desorption process shows a line that runs from the top of the figure down to the left. This was due to the movement of a small fluorescent speck with an intensity similar to ROI 1. Closer examination of the behavior of the small fluorescent specks revealed that they were mobile, coincident with the reductive desorption of the ssDNA surface. In total, four particles were

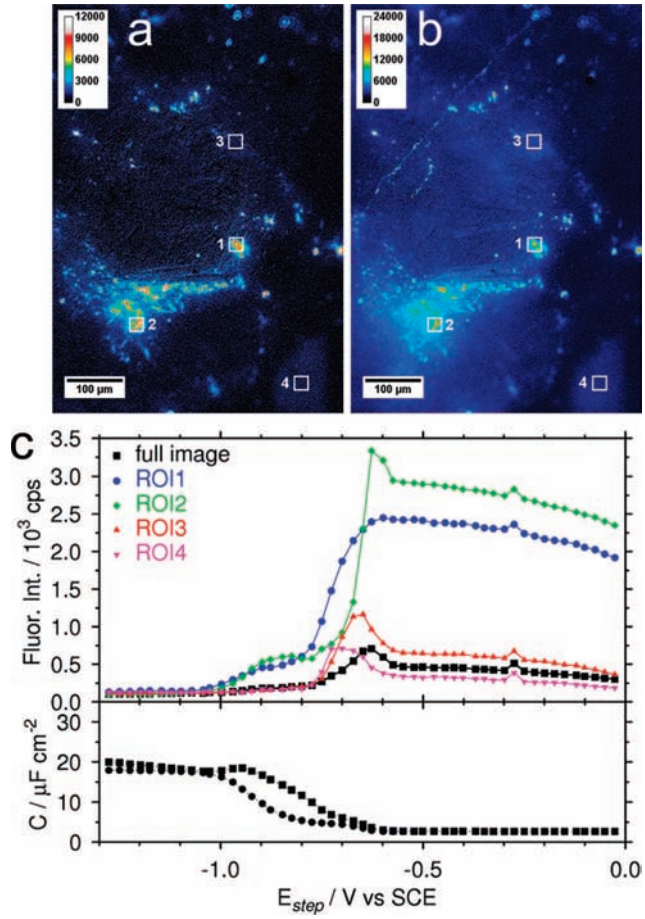


***Figure 6.*** Fluorescence images for the MCH/ssDNA-modified gold surface at (a) $E_{base}$ (0 mV) and (b) maximum of the $E_{step}$ images during desorption. (c) Fluorescence intensity (top) measured (at $E_{step}$) for the whole image and selected ROIs (50 $\mu$m × 50 $\mu$m), and capacitance (bottom) measured at $E_{step}$ (■) and $E_{base}$ (●) after the $E_{step}$ potential excursion. The intensity of fluorescence is rendered as a range of colors, shown in the color−intensity bar.

observed to move across the surface after desorption was initiated. These specks were tracked using the ImageJ plugin MTrackJ.[44] The trajectory for four of these particles is shown in Figure 7, illustrating that the particles move from right to left toward the bottom of the image. We are unsure of the reason for this, but we speculate that the particle is moving toward the counter electrode. It is clear that the particles start moving only when the potential is sufficiently negative. In one case the particle (1) starts to move at −650 mV, while others (3 and 4) start to move at −825 mV. The particles remain intact and do not break apart, suggesting it may be a DNA crystallite that is physisorbed onto the MCH layer and may become active once the MCH layer starts to reductively desorb. There are other similarly sized particles (diameter of 3−5 $\mu$m) that also move toward the bottom-left corner (see the movie available as Supporting Information). The velocity of the particles range from 0 to 10 $\mu$m/s and do not correlate strongly with the applied potential. The forces holding the particle to the surface are not known but may involve a combination of electrostatic or interfacial tension forces that are controlling the particle motion/friction on the surface. This observation is significant, as is demonstrates that these highly fluorescent regions on the DNA-

(44) Meijering, E. *MTrackJ v1.2.0.*

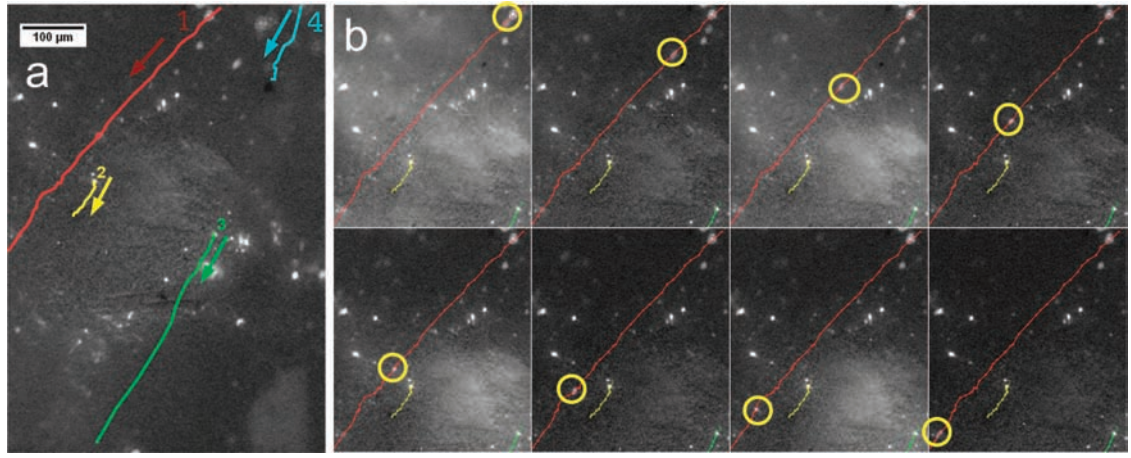


***Figure 7.*** (a) Traces for four mobile particles observed during the reductive desorption of the modified MCH/ssDNA surface. Each trace represents one particle and is superimposed on the $E_{base}$ fluorescence image. All particles start at the top right of the image and move toward the bottom left. Not shown are the different initiation potentials. (b) A montage of images showing the progression of particle 1 outlined with a circle.

modified surfaces are trapped crystallites that are electrochemically manipulated and given rise to unexpected behaviors and probably decrease the hybridization efficiency. Presently unanswered is whether these particles are counted in the DNA surface concentration measured using the $[Ru(NH_3)_6]^{3+}$ electrochemical assay.

**3.7. MCH/dsDNA Potential Modulation from 0 to −400 mV.** The modified gold surface created using dsDNA after exposure to MCH produced a surface that was 10 times brighter (at $E_{base}$) and contained ~3 times the density of strands when compared to the ssDNA-modified surface. Duplex DNA is more rigid than the ssDNA and would extend further from the surface, resulting in more than a proportional increase in fluorescence. Very few local hot spots (Figure 5b) were observed on this surface, confirming the previous result that dsDNA is less prone to aggregation and nonspecific adsorption. The potential driven fluorescence modulation was 20%, noticeably smaller than the MCH/ssDNA example, presumably due to an increase in packing and that dsDNA may not be flexible enough to reach the maximum quenching possible, decreasing the total change in fluorescence. The regional variation in the degree of modulation ranged from 25% to 10% with the vast majority of areas showing a change in fluorescence with potential. Again, the regions with the highest $E_{base}$ fluorescence exhibited the smallest proportional increase in fluorescence, suggesting higher dsDNA density in these regions.

**3.8. MCH/dsDNA Reductive Desorption.** The electrochemical removal of the MCH/dsDNA layer was studied using fluorescence and capacitance measurements, as shown in Figure 8. Fluorescence and capacitance indicate that desorption began at −625 mV, similar to the MCH/ssDNA layer and the dsDNA/MCH surface. This is in contrast to the ssDNA/MCH layer, where a significantly more negative potential was required, as measured using fluorescence and capacitance. This similarity in potential suggests that desorption of the MCH layer controls the removal process. The capacitance does indicate a small positive shift (25−50 mV) for the MCH/dsDNA surface as compared to the MCH/ssDNA surface for the initial increase due to thiol removal. The fluorescence intensity−potential dependence is more uniform than compared to the MCH/ssDNA surface, all regions showing an increase in fluorescence corresponding to removal of the thiol and a decrease to zero at the most negative $E_{step}$ potentials. Again, the trend is showing that

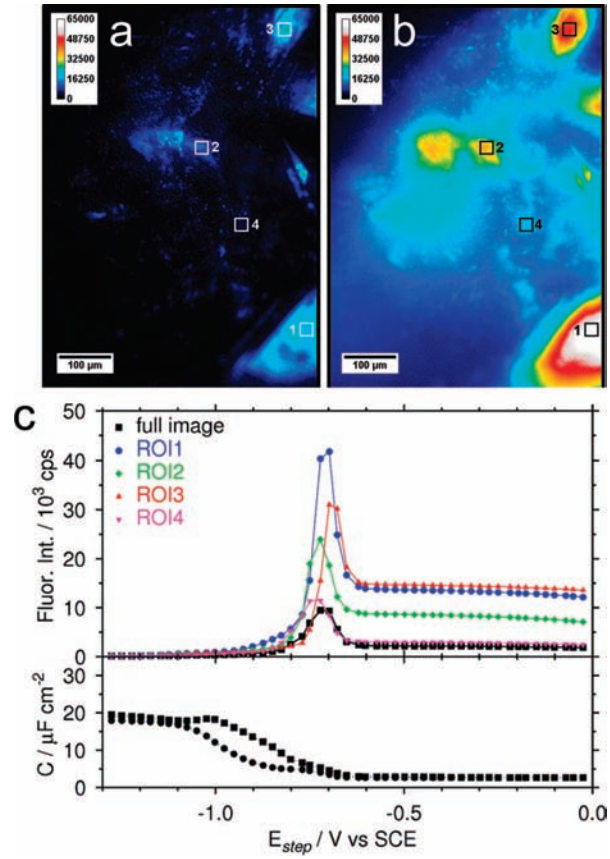


***Figure 8.*** Fluorescence images for the MCH/dsDNA-modified gold surface at (a) $E_{base}$ (0 mV) and (b) maximum of the $E_{step}$ images during desorption. (c) Fluorescence intensity (top) measured (at $E_{step}$) for the whole image and selected ROIs (50 $\mu$m × 50 $\mu$m), and capacitance (bottom) measured at $E_{step}$ (■) and $E_{base}$ (●) after the $E_{step}$ potential excursion. The intensity of fluorescence is rendered as a range of colors, shown in the color−intensity bar.

the most intense regions at $E_{base}$ yield a proportionally smaller change in the fluorescence during desorption. In contrast to the dsDNA/MCH layers, the desorption occurs over a small potential range and the change in fluorescence does not show a significant shoulder at negative potential. The modified surface produced using this method yields surfaces that are homoge-

neous in terms of the removal of the thiol layer, but the coverage of DNA is variable and depends on the surface under study.

## 4. Conclusions

Gold surfaces were modified through the creation of SAMs of fluorescently tagged DNA backfilled with MCH following commonly used procedures and were characterized using electrochemical methods coupled with fluorescence imaging. These surfaces, whether prepared with ssDNA or dsDNA, resulted in heterogeneous surface coverage with hot spots of intense fluorescence from a presumably quenched fluorescent species. The changes in fluorescence due to potential modulation were inconsistent; the intense fluorescence regions were suggested to be due to aggregated structures that were physisorbed onto the modified surface. The hot spots disproportionately (on an absolute scale) responded to electrochemical perturbations that may indicate problems for DNA sensors based on fluorescence intensity measurements. The increase in fluorescence due to reductive desorption demonstrated that the surface was completely modified, though variable across the surface. The dsDNA-modified surfaces did not show significant heterogeneity, though hot spots were still evident on the surface. A modified preparation method was used that initially treated the surface with MCH followed by immersion in the ssDNA or dsDNA modification solutions. The thiolated DNA modified the MCH-coated Au surface by way of a thiol-place exchange reaction or through pinholes in the MCH SAM. These surfaces were of a much lower surface concentration of DNA but displayed little to no hot spots (especially true for the dsDNA) and the fluorescence could be strongly modulated with changes in electrode potential, ideal for monitoring hybridization events. The movement of small highly fluorescent specks was noted, providing clear evidence of physisorbed crystallites of fluorescent DNA strands. Overall, gold surfaces modified by thiolated DNA SAMs are significantly heterogeneous, which results in regional differences in the intensity of fluorescence whether unbiased or under potential modulation. Our findings outline the importance of considering surface heterogeneity when designing DNA sensors and of involving microscopic characterization using methods like the electrochemical in situ fluorescence imaging technique.

**Acknowledgment.** Funding from NSERC (Canada) supports this work. A.K.H.C. gratefully acknowledges financial support for his graduate studies from NSERC and SFU. We would like to thank Dr. Yunchao Li for helpful discussions and advice and the UBC Chemistry Shops for technical support.

**Supporting Information Available:** A schematic of the experimental setup is provided. In addition, movies created with the fluorescence images taken at $E_{step}$ extracted from the potential step experiments for the four interfaces discussed are available. A movie of the particle motion described in section 3.6 is also available. The fluorescence intensity modulation for a variety of regions on the MCH/dsDNA interface described in section 3.7 is detailed. This material is available free of charge via the Internet at http://pubs.acs.org.

JA808696P